Macromolecules 1988, *21*, 2469–2474

some amounts of the cooled phase, the high tensile stress lowers the free energy of this trans phase compared to that under free tension because of the occurrence of the phase transition to the thermodynamically more stable trans form. The crossing of the transition point shifts to the higher temperature side. The T_c, plotted against tensile stress σ, is expected to change as illustrated in the lower half-side of Figure 15b. This is consistent with the experimental result shown in Figures 9 and 10.

Conclusion

In the present paper we have discussed the effect of tensile stress on the ferroelectric phase transition of the VDF–TrFE copolymer system based on the measurement of the thermally induced dimensional change along the chain direction.

The tensile stress lowers the crystalline transition point at a rate of ca. $-4 \sim -7$ °C/MPa. The X-ray diffraction measurement under tension supported this conclusion. An application of the modified Clausius–Clapeyron equation was found to be useful for interpretation of the phenomenon. In a high tensile stress region, on the other hand, the structurally disordered cooled phase is forced to transform to the regular low-temperature phase, resulting in the rather high-temperature shift of the transition point for VDF 52 and 65% samples.

What happens when the tensile force is applied in the direction perpendicular to the chain axis? The experimental results will be reported in the next paper of this series.

Acknowledgment. We are grateful to Daikin Kogyo Company, Ltd., Japan for supplying the samples of VDF–TrFE copolymers as well as for use of their X-ray diffractometer. This work was supported in part by a Grant-in-Aid on Special Project Research for "Organic Thin Films for Information Conversion" from the Ministry of Education, Science and Culture, Japan.

Registry No. (VDF)(TrFE) (copolymer), 28960-88-5.

References and Notes

(1) Tashiro, K.; Takano, K.; Kobayashi, M.; Chatani, Y.; Tadokoro, H. *Polymer* **1981**, *22*, 1312.
(2) Tashiro, K.; Takano, K.; Kobayashi, M.; Chatani, Y.; Tadokoro, H. *Polymer* **1984**, *25*, 195.
(3) Tashiro, K.; Takano, K.; Kobayashi, M.; Chatani, Y.; Tadokoro, H. *Ferroelectrics* **1984**, *57*, 297.
(4) Lovinger, A. J.; Davis, G. T.; Furukawa, T.; Broadhurst, M. G. *Macromolecules* **1982**, *15*, 323.
(5) Lovinger, A. J.; Davis, G. T.; Furukawa, T.; Broadhurst, M. G. *Polymer* **1983**, *24*, 1225, 1233.
(6) Ii, T.; Tashiro, K.; Kobayashi, M. *Macromolecules* **1986**, *19*, 1809.
(7) Tashiro, K.; Kobayashi, M. *Polymer* **1986**, *27*, 667.
(8) Choy, C. L.; Chen, F. C.; Young, K. *J. Polym. Sci., Polym. Phys. Ed.* **1981**, *19*, 335.
(9) Orchard, G. A. J.; Davis, G. R.; Ward, I. M. *Polymer* **1984**, *25*, 1203.
(10) Choy, C. L.; Leung, W. P.; Ong, E. L. *Polymer* **1985**, *26*, 884.
(11) Koizumi, N.; Murata, Y.; Oka, Y. *Jpn. J. Appl. Phys.* **1984**, *23*, L324.
(12) Sawatari, C.; Matsuo, M. *Macromolecules* **1986**, *19*, 2726.
(13) Koizumi, N.; Haikawa, N.; Habuka, H. *Ferroelectrics* **1984**, *57*, 99.
(14) Murata, Y.; Koizumi, N. *Rep. Progr. Polym. Phys. Jpn.* **1987**, *30*, 363.
(15) Tashiro, K.; Nishimura, S.; Kobayashi, M. *Rep. Progr. Polym. Phys. Jpn.* **1987**, *30*, 355.
(16) Tashiro, K.; Kobayashi, K.; Tadokoro, H. *Macromolecules* **1977**, *10*, 731.
(17) Tasaka, S.; Miyata, S. *Ferroelectrics* **1981**, *32*, 17.
(18) Miyasaka, K.; Makishima, K. *Kobunshi Kagaku* **1966**, *23*, 785.
(19) Ii, T.; Tashiro, K.; Kobayashi, M.; Tadokoro, H. *Proc. Am. Chem. Soc., Div. Polym. Mater. Sci. Eng.* **1986**, *55*, 826.

Effect of Crystallization Condition on the Ferroelectric Phase Transition in Vinylidene Fluoride/Trifluoroethylene (VF_2/F_3E) Copolymers

Hajime Tanaka,* Hideyuki Yukawa,[†] and Toshio Nishi

Department of Applied Physics, Faculty of Engineering, The University of Tokyo, Bunkyo-ku, Tokyo 113, Japan. Received November 10, 1987

ABSTRACT: We report the effects of crystallization temperature on thermal properties of the ferroelectric transitions of random copolymers of vinylidene fluoride (VF_2) and trifluoroethylene (F_3E). We find that the Curie point decreases as the crystallization temperature increases. In the copolymer containing 65 mol % VF_2, two peaks corresponding to the Curie transitions are observed only when the copolymer is crystallized in a paraelectric phase. The results clearly indicate that the crystalline structure of the ferroelectric phase strongly depends on the crystallization temperature, especially on whether a copolymer is crystallized above or below the Curie point. This can be understood by the imperfection of the solid–solid transformation of the crystalline structure from the paraelectric to the ferroelectric phase. A phase diagram containing two kinds of ferroelectric phases has been proposed.

Introduction

Since the discovery of the ferroelectric phase transition in random copolymers of vinylidene fluoride (VF_2) and trifluoroethylene (F_3E),[1–7] the ferroelectric transition has been extensively studied by many researchers.[1–13] The crystalline structures have been studied in detail by X-ray diffraction measurements, and the structural change accompanied by the ferroelectric phase transition has been made clear.[8–13] The transition from the ordered ferroelectric phase to the disordered paraelectric phase is ascribed to the structural and conformational change of molecular chains inside the crystal. Spectroscopic studies using Raman scattering and infrared absorption also support the conformational change by the transition.[11–13]

[†] Current address: Mazda Motor Corporation, Hiroshima City, Hiroshima, Japan.

0024-9297/88/2221-2469$01.50/0

In the ferroelectric low-temperature phase, a chain in the crystal has a planar all-trans conformation, and the packing of chains in the ferroelectric phase (point group $m2m$) is analogous to that of the ferroelectric β-phase of poly(vinylidene fluoride) (PVF_2). The degree of order of the crystal depends on VF_2 content. Copolymers of lower VF_2 content have a less ordered crystalline structure. In the paraelectric high-temperature phase, on the other hand, the molecular chain has a partly disordered conformation consisting of irregular TG, T$\bar{G}$, and TT sequences and is packed on an expanded hexagonal lattice.[10] The ferroelectric phase transition of copolymers is thought to be first order from both the large thermal hysteresis and the coexistence of two crystalline phases in a certain temperature region.

The Curie transition is ascribed to the order–disorder transition of the crystalline phase. Generally, a crystalline polymer is composed of crystalline lamellae, an interface, and an amorphous phase. The crystalline structure strongly depends on the crystallization condition. For example, the crystallinity and the thickness of crystalline lamellae are affected by the crystallization temperature, T_{cry}. Therefore, the crystallization condition should have an effect on the ferroelectric phase transition in a direct manner or an indirect manner. This effect is one of the unique characteristics of ferroelectric polymers in contrast to the other ferroelectric materials such as single crystals and ceramics. Recently, the effect of solution history and annealing on the ferroelectric transition has been studied by Green et al.[14] and Fernandez et al.[15] To our knowledge, however, there have been no systematic studies on the effects of T_{cry} on the ferroelectric phase transition. In this paper, we focus our attention on the effects of T_{cry} on the ferroelectric phase transition and the crystallization.

Experimental Section

Samples used were VF_2/F_3E copolymers furnished by Daikin Kogyo Co. Ltd. We used three samples with different VF_2 contents. They have 52, 65, and 73 mol % VF_2 contents. A sample was sealed in an aluminum pan for the differential scanning calorimetry (DSC) measurement. Then it was placed on the hot stage of the temperature controller (Mettler FP52) for thermal treatment. The sample was kept at 180 °C in the melt to eliminate any trace of crystals. Then it was quenched to a crystallization temperature (T_{cry}) within a sufficiently short time and isothermally crystallized for a day. In the case of $T_{cry} < 80$ °C, the sample was immersed directly in liquid N_2 from melt to avoid crystallization above T_{cry}, and then it was isothermaly crystallized at T_{cry} (above the glass transition temperature, T_g) by setting it on a temperature-controlled hot stage.

All the DSC measurements were carried out with a Perkin-Elmer DSC1-B instrument at the scan speed of 8 °C/min for both heating and cooling measurements.

Results

Figures 1, 2, and 3 show a T_{cry} dependence of the endothermic curves for VF_2/F_3E (52/48), VF_2/F_3E (65/35), and VF_2/F_3E (73/27), respectively. The peak at lower temperature corresponds to the ferroelectric phase transition, and the peak at higher temperature corresponds to the melting point (T_m) of the crystalline phase. The peak positions of the Curie transition shift to lower temperature with an increase in T_{cry}. On the other hand, the melting points increase with T_{cry} as in the usual semicrystalline polymers.

In VF_2/F_3E (65/35) (see Figure 2), two peaks corresponding to the Curie transition are observed in the case of $T_{cry} > 100$ °C. This double-transition behavior was also observed by Davis et al.[16] in the as-received sample with the same VF_2 content. As T_{cry} increases, the lower temperature peak grows and the higher temperature peak disappears. In VF_2/F_3E (73/27) (see Figure 3), two peaks corresponding to the Curie transition are also observed for the sample crystallized at $T_{cry} = 140$ °C.

Figure 4 shows exothermic curves for three copolymers cooled at a rate of 8 °C/min. The dip at higher temperature corresponds to crystallization and that at lower temperature corresponds to the ferroelectric phase transition from the paraelectric to the ferroelectric phase. In VF_2/F_3E (65/35) and VF_2/F_3E (73/27), two peaks corre-

Table I
Dependence of Endothermic and Exothermic Characteristic Temperatures on the Crystallization Temperature (T_{cry}, °C) in VF_2/F_3E (52/48) Copolymer[a]

T_{cry}	$T_{t\uparrow}^{L}$	$T_{t\uparrow}^{H}$	$T_{m\uparrow}$	$T_{m\downarrow}$	$T_{t\downarrow}^{H}$	$T_{t\downarrow}^{L}$
140	60.7		161.4	127.5		54.0
120	61.2		158.5			
100	62.0		157.0			
80	62.5		157.1			
50	62.7		157.3			
30	62.5		157.0			

[a] Peak temperatures corresponding to the Curie transitions in the heating process are defined as $T_{t\uparrow}^{L}$ (°C) and $T_{t\uparrow}^{H}$ (°C) for the lower and higher transitions, respectively. Those in the cooling process are defined as $T_{t\downarrow}^{L}$ (°C) and $T_{t\downarrow}^{H}$ (°C), melting temperature as $T_{m\uparrow}$ (°C), and temperature at which crystallization starts in the cooling process as $T_{m\downarrow}$ (°C).

Table II
Dependence of Endothermic and Exothermic Characteristic Temperatures on the Crystallization Temperature (T_{cry}, °C) in VF_2/F_3E (65/35) Copolymer. Definitions Are the Same as in Table I

T_{cry}	$T_{t\uparrow}^{L}$	$T_{t\uparrow}^{H}$	$T_{m\uparrow}$	$T_{m\downarrow}$	$T_{t\downarrow}^{H}$	$T_{t\downarrow}^{L}$
140	66.6	80.0	158.2	124.5	55.2	51.5
120	70.2	84.8	154.2			
100	70.0	85.9	152.6			
80		87.6	152.7			
50		91.7	152.8			
30		91.8	152.4			

Table III
Dependence of Endothermic and Exothermic Characteristic Temperatures on the Crystallization Temperature (T_{cry}, °C) in VF_2/F_3E (73/27) Copolymer. Definitions Are the Same as in Table I

T_{cry}	$T_{t\uparrow}^{L}$	$T_{t\uparrow}^{H}$	$T_{m\uparrow}$	$T_{m\downarrow}$	$T_{t\downarrow}^{H}$	$T_{t\downarrow}^{L}$
140	96.0	115.2	157.0	120.3	66.1	59.2
120		121.1	149.7			
100		121.4	148.7			
80		121.9	148.2			
50		123.3	147.5			
30		123.3	147.3			

Table IV
Dependence of Endothermic and Exothermic Heat on the Crystallization Temperature (T_{cry}, °C) in VF_2/F_3E (52/48) Copolymer[a]

T_{cry}	$Q_{t\uparrow}$	$Q_{m\uparrow}$	$Q_{m\downarrow}$	$Q_{t\downarrow}$
140	2.1	7.1	6.2	1.2
120	2.0	7.0		
100	2.0	6.8		
80	1.7	6.7		
50	1.6	6.6		
30	1.6	6.5		

[a] The heat of the ferroelectric transition in the heating and cooling processes is defined as $Q_{t\uparrow}$ (cal/g) and $Q_{t\downarrow}$ (cal/g), respectively. The heat of melting is defined as $Q_{m\uparrow}$ (cal/g) and the heat of crystallization as $Q_{m\downarrow}$ (cal/g).

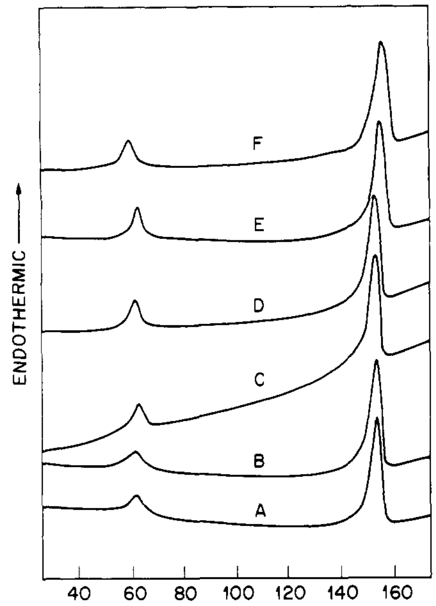

Figure 1. DSC scans from VF_2/F_3E (52/48) crystallized at various temperatures in the heating process. Curves A–F correspond to samples isothermally crystallized at 30, 50, 80, 100, 120, and 140 °C, respectively.

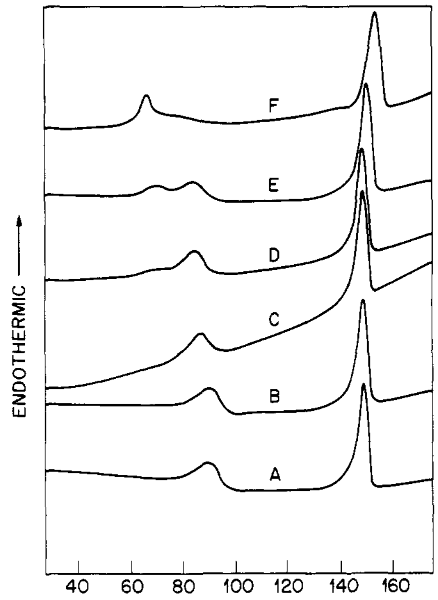

Figure 2. DSC scans from VF_2/F_3E (65/35) crystallized at various temperatures in the heating process. Curves A–F correspond to samples isothermally crystallized at 30, 50, 80, 100, 120, and 140 °C, respectively.

Table V
Dependence of Endothermic and Exothermic Heat on the Crystallization Temperature (T_{cry}, °C) in VF_2/F_3E (65/35) Copolymer. Definitions Are the Same as in Table IV

T_{cry}	$Q_{t\uparrow}$	$Q_{m\uparrow}$	$Q_{m\downarrow}$	$Q_{t\downarrow}$
140	4.1	7.0	6.7	2.9
120	3.9	6.6		
100	3.8	6.5		
80	3.6	6.2		
50	3.5	6.3		
30	3.4	6.1		

sponding to the phase transitions were also observed.

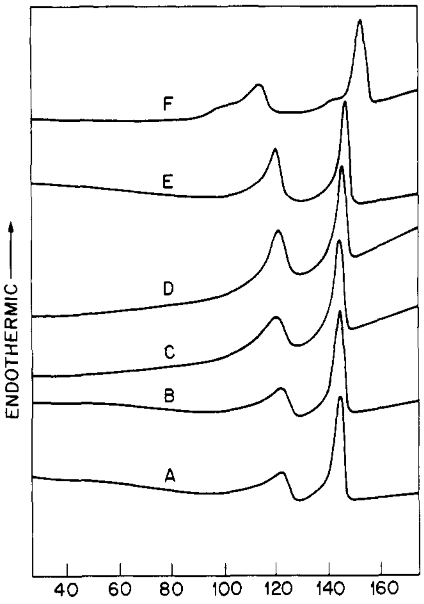

Figure 3. DSC scans from VF_2/F_3E (73/27) crystallized at various temperatures in the heating process. Curves A–F correspond to samples isothermally crystallized at 30, 50, 80, 100, 120, and 140 °C, respectively.

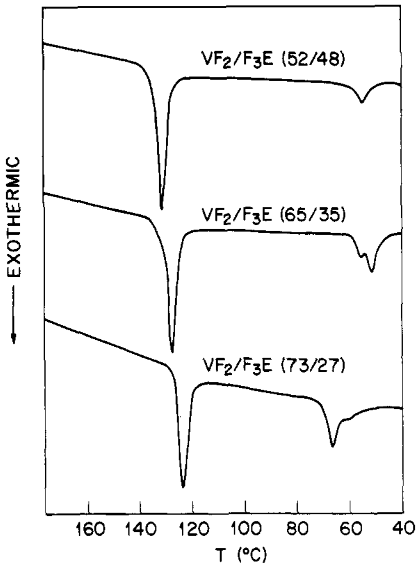

Figure 4. DSC scans from VF_2/F_3E (52/48, 65/35, 73/27) during cooling process.

Table VI
Dependence of Endothermic and Exothermic Heat on the Crystallization Temperature (T_{cry}, °C) in VF_2/F_3E (73/27) Copolymer. Definitions Are the Same as in Table IV

T_{cry}	$Q_{t\uparrow}$	$Q_{m\uparrow}$	$Q_{m\downarrow}$	$Q_{t\downarrow}$
140	5.0	7.1	7.1	4.2
120	5.1	7.0		
100	4.9	6.8		
80	4.5	6.6		
50	4.2	6.8		
30	3.9	6.6		

Tables I, II, and III show characteristic temperatures for the transition peak and the melting point. Tables IV, V, and VI show the heat of fusion of the transition and the melting processes. T_m and T_t denote the melting point temperature and the Curie transition temperature, respectively. $T_{m\uparrow}$ is determined from the high-temperature tail of the melting curve. T_t is defined as the peak position of the DSC curve corresponding to the transition. T_t^L and T_t^H represent the lower temperature peak and higher temperature peak, respectively. $T_{m\downarrow}$ is defined as the peak position of the exothermic peak corresponding to crystallization during the cooling process. Q_m and Q_t represent the heats of fusion of the melting and transition processes, respectively. The subscripts ↑ and ↓ indicate the quantities observed in the heating and cooling processes, respectively. These results will be discussed in the next section.

Discussion

A. Dependence of Curie Transition on Crystallization Temperature. In the case of VF_2/F_3E (52/48), T_t^L decreases slightly with an increase in T_{cry}. The peak corresponding to the ferroelectric phase transition has a single maximum in every case. As in the usual semicrystalline polymers, $T_{m\uparrow}$ increases as T_{cry} increases. Roughly, $Q_{m\uparrow}$ increases with T_{cry} and $Q_{t\uparrow}$ also increases with T_{cry}. $Q_{m\uparrow}$ is directly related to the crystallinity if the crystalline structure of the paraelectric phase is the same. However, the difference in VF_2 content may cause the difference in the crystalline structure of the paraelectric phase or its perfection. We also have to take into account the gradual crystallization during a heating process. At a heating rate of 8 °C/min, however, we may assume that it does not have a serious effect.

$Q_{t\uparrow}/Q_{m\uparrow}$ is not constant with regard to T_{cry}, indicating that the crystalline structure of the ferroelectric phase depends on T_{cry}, under the assumption that the crystalline structure of the paraelectric phase does not depend on T_{cry}.

The thickness of lamellae is roughly proportional to the inverse of the degree of undercooling ΔT ($=T_m - T_{cry}$). It should influence $T_{t\uparrow}$, $Q_{t\uparrow}$, and $T_{m\uparrow}$. It may also be closely related to the two-dimensional character of the transition and to the effect of the interface between the lamellae and the amorphous region on the transition.

The peak position of the transition $T_{t\uparrow}$, which is related to the Curie temperature T_c, decreases with T_{cry}. Generally, a more ordered state causes a higher transition temperature because an increase in the order stabilizes the ferroelectric phase. An increase in the thickness of lamellae reduces the interface effect and the two-dimentional character, which probably increases T_c.

The effect of T_{cry} on the Curie point can be explained as follows: When a copolymer is crystallized above T_c in a paraelectric phase, the crystal cannot transform perfectly to the ordered ferroelectric phase through the solid–solid transformation as it is cooled below T_c. The imperfection of this transformation is indicated by the fact that the X-ray diffraction pattern of the sample heated above T_c shows more disorder than that of the starting sample.[10] This imperfection in crystalline structure lowers the Curie point of a sample crystallized at higher temperature. As a copolymer is crystallized at higher temperature in a paraelectric phase, it crystallizes in a more complete paraelectric crystalline structure and the transformation to a complete ferroelectric phase becomes more difficult. As suggested by Lovinger,[17] this causes more conformational defects in the ferroelectric phase. This residual disorder derived from the paraelectric phase should become more apparent from studies of the dependence of the X-ray diffraction pattern on T_{cry}.

In the case of VF_2/F_3E (65/35), the dependence of $T_{t\uparrow}$, $T_{m\uparrow}$, and $Q_{m\uparrow}$ on T_{cry} is almost the same as in VF_2/F_3E (52/48). In this system, however, distinct transition peaks were observed. There is a clear tendency that the higher temperature peak height decreases and the lower temperature peak height increases with an increase in T_{cry}. This indicates that there exist two different types of crystalline structures in VF_2/F_3E (65/35). The appearance of the lower temperature peak critically depends on whether the copolymer is crystallized below T_c or above T_c. In the case of $T_{cry} < T_c$, there is no peak corresponding to the lower temperature peak, while a low-temperature peak appears at $T_{cry} > T_c$. At T_{cry} = 140 °C, the lower temperature peak is dominant.

In the case of VF_2/F_3E (73/27), the dependence of $T_{t\uparrow}$, $T_{m\uparrow}$, and $Q_{m\uparrow}$ on T_{cry} is qualitatively the same as the other two cases. In this case, there is almost one peak corresponding to the ferroelectric transition. In the case of T_{cry} = 140 °C, a small shoulder is observed in the lower temperature side of the main transition. The appearance of the shoulder can be explained by the same mechanism used for VF_2/F_3E (65/35) copolymer.

The ferroelectric phase seems to involve at least two types of crystalline structures. Here we define the crystalline structure having the lower transition temperature as the ferroelectric A (F_A) phase and that having the higher transition temperature as the ferroelectric B (F_B) phase.

In the case of VF_2/F_3E (52/48), the crystalline structure below T_c is the F_A phase which has a less ordered structure than the F_B phase. In the case of VF_2/F_3E (65/35), the crystalline phase formed above T_c contains the F_A phase and the F_B phase below T_c. Double peaks observed in DSC measurements reflect the ferroelectric phase transition of two different crystalline structures. The lower temperature peak corresponds to the ferroelectric phase transition of the F_A phase and the higher temperature peak to that of the F_B phase. In the case of VF_2/F_3E (73/27), the crystalline structure below T_c is thought to be mainly the F_B phase.

The higher transition temperature generally reflects a higher order of structure. Therefore, the order in the F_B phase is higher than that in the F_A phase. The dependence of T_t on T_{cry} is ascribed to the same origin. That is, the structure crystallized at higher temperature, especially above T_c, contains more disordered conformations, which account for the structural hysteresis of the ferroelectric phase transition.

The F_A phase is the less ordered ferroelectric phase into which a copolymer is transformed from the paraelectric phase after the crystallization in the paraelectric phase, while the F_B phase is the more ordered ferroelectric phase. In VF_2/F_3E (52/48), we observe only the F_A phase. It is not clear at the present stage which of the following two mechanisms is responsible for this: (a) This copolymer is difficult to crystallize in a ferroelectric phase because of a low T_c, and it crystallizes in a paraelectric phase under the usual crystallization conditions. The imperfect transformation from the paraelectric to ferroelectric phase causes the appearance of the A phase. (b) This copolymer contains more defects than the other two. This makes the formation of the ordered F_B phase difficult.

It should be mentioned that it might be possible to interpret the double-transition behavior by assuming the existence of an intermediate transient phase. That is, the lower temperature peak is caused by the transformation from the F_B phase to the F_A phase, and the higher temperature peak is caused by the transformation from the F_A phase to the paraelectric phase. Figure 5 schematically shows the possible types of the transition for VF_2/F_3E (65/35). Model a assumes that two kinds of ferroelectric phases coexist at room temperature when $T_{cry} > T_c$. On the other hand, models b and c assume that there is only one kind of ferroelectric phase at room temperature. In models b and c, the F_A phase may be in a metastable state. The models can be realized by a system with Gintzburg–Landau-type free energy which has at least four minima at the non-zero-order parameter at a certain temperature.

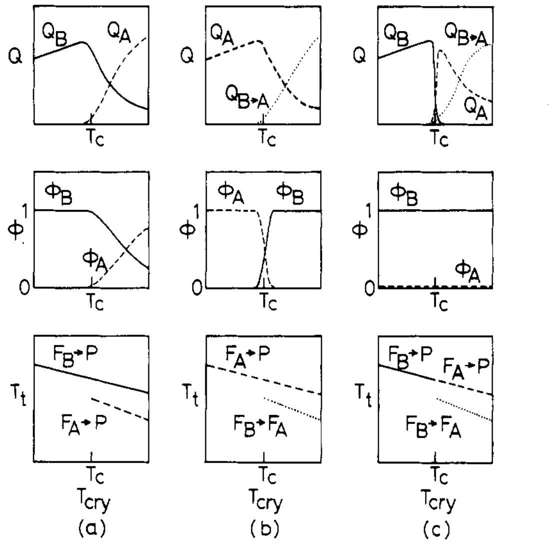

Figure 5. Three models for a ferroelectric transition in VF_2/F_3E (65/35). In case a, two kinds of ferroelectric phases (F_A and F_B) transform into the paraelectric phase P independently, and F_A appears only when $T_{cry} > T_c$. In case b, the higher temperature transition is assigned to the transition from F_A to P and the lower temperature transition to the transition from F_B to F_A. In case c, the higher temperature transition is assigned to the transition from F_B to P in the case $T_{cry} < T_c$ and to that from F_A to P in the case $T_{cry} > T_c$, respectively. The lower temperature transition is assigned to the transition from F_B to F_A. In the lower column, the dependence of the transition temperature (T_t) on the crystallization temperature (T_{cry}) is shown. In the middle column, the fraction of the F_B phase (ϕ_B) and that of the F_A phase (ϕ_A) are shown as a function of T_{cry}. In the upper column, the heat of the transition (Q) is shown against T_{cry}.

In this case, the free energy should include the order parameter (polarization) to the eighth power.

In case a, there are two types of ferroelectric phases which transform to the paraelectric phase independently. The system crystallized above T_c is a mixture of the F_A phase and the F_B phase below T_c, in this case. In cases b and c, there exists an intermediate (F_A) phase in the system crystallized above T_c. In model b, the ferroelectric phase at room temperature is the F_B phase at $T_{cry} < T_c$ and the F_A phase at $T_{cry} > T_c$. This sharp transition at $T_{cry} = T_c$ is unrealistic. In model c, on the other hand, the behavior of the heat of fusion (Q) is unrealistic for the same reason. It is also strange that the transition temperature of F_B is smoothly connected to that of F_A at $T_{cry} = T_c$ in model c (see Figure 5).

Furthermore, according to the models which assume an intermediate phase, it is difficult to explain the dependence of $T_{t\uparrow}$ on T_{cry} and the behavior in VF_2/F_3E (73/27) where only a high-temperature peak is mainly observed. It is also difficult to explain the strong correlation between the appearance of a low-temperature peak and whether or not T_{cry} is higher than T_c. Therefore, at the present stage, we think that the models which assume the intermediate phase are not suitable to explain the phenomena.

B. Cooling Process. In the cooling process (see Figure 4), the crystallization temperature is higher for the sample containing a lower VF_2 content, and this is consistent with a melting point dependence on VF_2 content. Except for VF_2/F_3E (52/48), there are two peaks for the Curie transition. This is consistent with the coexistence of two types of crystalline forms in VF_2/F_3E (65/35) and VF_2/F_3E (73/27). It should be noted that the lower temperature peak position of VF_2/F_3E (65/35) is lower than the peak position of VF_2/F_3E (52/48). The transition from the paraelectric phase to the ferroelectric phase is sharper and more symmetrical than that from the ferroelectric phase to the paraelectric phase. The appearance of two transition peaks indicates the following two possibilities: (1) The transition from the paraelectric to the ferroelectric phase occurs in two ways. Part of the paraelectric phase transforms into the F_B phase, and then the remainder of the paraelectric phase transforms into the F_A phase. (2) The transition occurs through an intermediate phase. The paraelectric phase transforms to the F_A phase, and then the F_A phase transforms to the F_B phase. A clear understanding of this process is very important; however, at the present stage, it is difficult to determine which mechanism is correct. The larger peak height of the higher temperature peak in VF_2 richer copolymers suggests that mechanism 1 is most likely.

$Q_{t\downarrow}$ is smaller than $Q_{t\uparrow}$, which is consistent with the imperfection of the transformation from the paraelectric phase to the ferroelectric phase.

C. Effect of VF_2 Content. Next we briefly discuss the effect of VF_2 content. The melting point $T_{m\uparrow}$ increases with a decrease in VF_2 content. This is evident from the melting point depression in the copolymer as a function of VF_2 content. The Curie point (T_c) increases with an increase in VF_2 content. A higher T_c at a higher VF_2 content suggests that the higher VF_2 makes the F_B phase more stable. $Q_{t\uparrow}$ increases with an increase in VF_2 content. $Q_{m\uparrow}$ does not depend strongly on VF_2 content. This does not necessarily mean comparable crystallinity because crystalline order should depend on VF_2 content. The value of $Q_{t\uparrow}$ is related to the energy difference between the two crystalline structures. A small $Q_{t\uparrow}$ suggests a small energetic difference between the ferroelectric and paraelectric phases. This leads to the reasonable conclusion that a larger VF_2 content increases both the order of the ferroelectric structure and the energy differential of the transition. This is consistent with a stronger first-order character of the transition and a higher T_c in the copolymer with a higher VF_2 content.

The transition is narrowest and most symmetrical in VF_2/F_3E (52/48). The broadness of the transition also depends on VF_2 content. The half-height width of the transition peak of the copolymers crystallized below the Curie point is about 6, 10, and 12 °C for the copolymers with VF_2 contents of 52, 65, and 73 mol %, respectively. The peak broadness reflects the first-order character of the transition. The second-order transition involves no coexistence of ordered and disordered phases, and the transition is sharp. The ordered and disordered phases in the first-order transition coexist in a certain temperature range, making the transition broader. In this sense, the transition in the copolymer with 52 mol % VF_2 is almost second order. The small thermal hysteresis and the anomaly in the dynamic quantities observed by an ultrasonic measurement[18] and NMR[19] also support the above observation.

D. Phase Diagram. Finally we discuss the phase diagram of this copolymer mainly in the heating process. Tashiro et al.[11] reported the phase diagrams for this copolymer. They grouped the ferroelectric phase into two kinds, the cooled phase (the less ordered ferroelectric phase) and the low-temperature phase (the more ordered ferroelectric phase) from a crystallographical standpoint. The former seems to be close to the F_A phase, and the latter is close to the F_B phase. According to their phase diagram, in the vicinity of a VF_2 content of 65 mol %, the low-temperature phase transforms to the paraelectric phase through an intermediate phase, the cooled phase. However, the thermal behavior observed here can be ex-

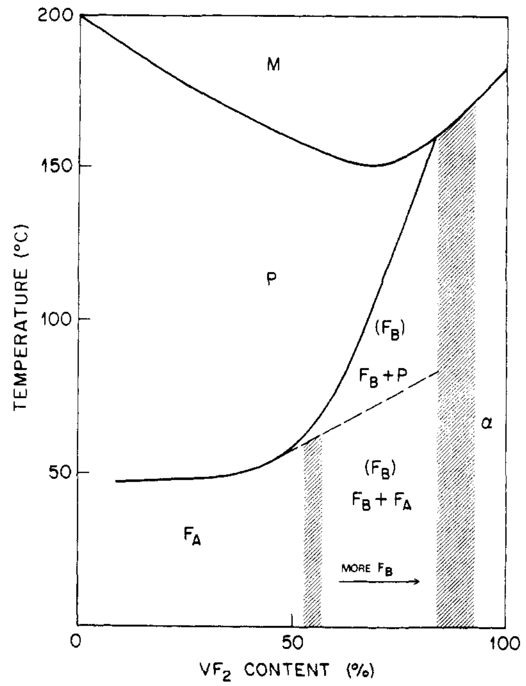

Figure 6. Schematic phase diagram of VF_2/F_3E copolymers crystallized from melt. M, melt; P, paraelectric phase; F_A, ferroelectric A phase (less ordered ferroelectric phase); F_B, ferroelectric B phase (more ordered ferroelectric phase); α, α-form crystal. Shaded area means the diffuse transition. As described in the text, these features depend on the crystallization conditions. In the case $T_{cry} < T_c$, there is no transition drawn by the dashed line, and the crystal has the F_B phase both above and below the dashed line as indicated in the parentheses.

plained better by the following mechanism than by assuming the existence of an intermediate phase: Both F_A and F_B phases coexist at room temperature if the copolymer is crystallized above T_c, and the two kinds of ferroelectric phase (F_A and F_B) transform into the paraelectric phase independently at different temperatures. We propose the schematic phase diagram of $P(VF_2/F_3E)$ in Figure 6.

The F_B phase is probably efficiently obtained by crystallization below T_c because of a kinetic reason. In the case $T_{cry} > T_c$, the cooling rate might affect the formation of the F_A phase. The potential barrier for the transformation between the F_A phase and F_B phase may be large, and the transformation may be possible only through the paraelectric phase.

Conclusions

We find that the ferroelectric phase transition is strongly affected by crystallization temperature. There are two kinds of ferroelectric phases: the less ordered F_A phase and the more ordered F_B phase. The F_B phase has a higher T_c. The F_B phase only appears when copolymers are crystallized below the Curie point. This probably occurs when a system crystallized in the paraelectric structure is not fully transformed to the ordered ferroelectric structure in solid state by decreasing temperature. Only when the copolymer crystallizes directly to form a ferroelectric phase can it crystallize in ordered fashion (F_B phase).

In a practical sense, we may achieve better ferroelectric properties when a copolymer is crystallized below the Curie point. A comparison between a sample annealed at a certain temperature above T_c and that crystallized at the same temperature is also interesting. X-ray studies will give direct information on the appearance of two peaks in the Curie transition and the structures of two kinds of ferroelectric phases.

Acknowledgment. We are indebted to Daikin Kogyo Co. Ltd. for kindly providing us samples (VF_2/F_3E copolymers). We are also grateful to Dr. A. J. Lovinger at AT&T Bell Laboratories for valuable discussions. This work was partly supported by a Grant-in-Aid from the Ministry of Education, Science and Culture, Japan.

Registry No. $(VF_2)(F_3E)$ (copolymer), 28960-88-5.

References and Notes

(1) Yagi, T.; Tatemoto, M.; Sako, J. I. *Polym. J.* **1980**, *12*, 209.
(2) Kitayama, T.; Ueda, T.; Yamada, T. *Ferroelectrics* **1980**, *28*, 301.
(3) Furukawa, T.; Date, M.; Fukada, E.; Tajitsu, Y.; Chiba, A.; *Jpn. J. Appl. Phys.* **1980**, *19*, L109.
(4) Tajitsu, Y.; Chiba, A.; Furukawa, T.; Date, M.; Fukada, E. *App. Phys. Lett.* **1980**, *36*, 286.
(5) Higashihata, Y.; Sako, J.; Yagi, T. *Ferroelectrics* **1981**, *32*, 85.
(6) Yamada, T.; Ueda, T.; Kitayama, T. *J. Appl. Phys.* **1981**, *52*, 948.
(7) Furukawa, T.; Johnson, G. E.; Bair, H. E.; Tajitsu, Y.; Chiba, A. *Ferroelectrics* **1981**, *32*, 61.
(8) Davis, G. T.; Furukawa, T.; Lovinger, A. J.; Broadhurst, M. G. *Macromolecules* **1982**, *15*, 323, 329.
(9) Lovinger, A. J.; Furukawa, T.; Davis, G. T.; Broadhurst, M. G. *Ferroelectrics* **1983**, *50*, 553.
(10) Lovinger, A. J.; Furukawa, T.; Davis, G. T.; Broadhurst, M. G. *Polymer* **1983**, *24*, 1225, 1233.
(11) Tashiro, K.; Takano, K.; Kobayashi, M.; Chatani, Y.; Tadokoro, H. *Ferroelectrics* **1984**, *57*, 297.
(12) Tashiro, K.; Kobayashi, M. *Jpn. J. Appl. Phys.* **1985**, *24*, 24-2,873.
(13) Green, J. S.; Rabe, J. P.; Rabolt, J. F. *Macromolecules* **1986**, *19*, 1725.
(14) Green, J. S.; Farmer, B. L.; Rabolt, J. F. *J. Appl. Phys.* **1986**, *60*, 2690.
(15) Fernandez, M. V.; Suzuki, A.; Chiba, A. *Macromolecules* **1987**, *20*, 1806.
(16) Davis, G. T.; Broadhurst, M. G.; Lovinger, A. J.; Furukawa, T. *Ferroelectrics* **1984**, *57*, 73.
(17) Lovinger, A. J. *Macromolecules* **1985**, *18*, 910.
(18) Tanaka, H.; Yukawa, H.; Nishi, T., unpublished results.
(19) Tanaka, H.; Yukawa, H.; Nishi, T., unpublished results.